

Strangeness Modes in Nuclei Tested by Anti-Neutrinos

E.E. Kolomeitsev^{a*}, and D.N. Voskresensky^{a,b†}

^a*Gesellschaft für Schwerionenforschung, Planckstr. 1, 64291 Darmstadt, Germany*

^b*Moscow Engineering Physical Institute, Kashirskoe shosse 31, 115409 Moscow, Russia*

Abstract

Production of negative strangeness in reactions of inelastic anti-neutrino scattering on a nucleus provides information on the modification of strange degrees of freedom in nuclear matter. We calculate cross-sections of the reaction channels $\bar{\nu}_{e(\mu)} \rightarrow e^+(\mu^+) + K^-$ and $\bar{\nu}_{e(\mu)} + p \rightarrow \Lambda + e^+(\mu^+)$ and investigate their sensitivity to the medium effects. In particular, we consider effects induced by the presence of a low-energy excitation mode in the K^- spectrum, associated with the correlated Λ -particle and proton-hole states, and the renormalization of the weak interaction in medium. In order to avoid double counting, various contributions to anti-neutrino scattering are classified with the help of the optical theorem, formulated within the non-equilibrium Green's function technique.

PACS: 25.30.Pt, 21.65.+f, 14.40.Aq

*e-mail: E.Kolomeitsev@gsi.de

†e-mail: voskre@rzri6f.gsi.de

I. MOTIVATION.

The knowledge of strange particle properties in nuclear matter is of importance for the many interesting phenomena. For example, hyperonization and K^-/\bar{K}^0 condensation in neutron stars [1–3], enhancement of K^- yield in heavy-ion collisions [4,5], scattering of strange particles on nuclei [6], and level shifts in kaonic atoms [7] are discussed recently in the literature. To gain new information it is desirable to design experiments, which directly probe the in-medium modification of strange particle properties. In Ref. [8] R.F. Sawyer suggested to study the reaction $\bar{\nu}_{e(\mu)} \rightarrow e^+(\mu^+) + K^-$, decay of an anti-neutrino in a nucleus into a positive lepton and an in-medium kaon. This process can occur only if a kaon with space-like momentum can propagate in nuclear matter and, therefore, would demonstrate that the kaon spectrum is modified in medium compared to its vacuum form. In Ref. [8] R.F. Sawyer described the K^- spectrum in terms of a single quasiparticle mode, $\omega_{K^-}(k)$, determined by attractive scalar and vector potentials. Consequently, for momenta exceeding a critical value k_c , the spectrum is soft with $\omega_{K^-}(k) \leq k$. Hence, for an anti-neutrino with the energy $E_{\bar{\nu}} > k_c$ the above reaction channel opens. The value of the critical momentum is $k_c \approx 2000 \text{ MeV} - \frac{4}{3} \Sigma_{KN}$, where Σ_{KN} is the kaon–nucleon Σ -term. Using the range of Σ_{KN} from Ref. [1], $200 \text{ MeV} < \Sigma_{KN} < 400 \text{ MeV}$, we estimate the critical momentum as $1500 \text{ MeV} < k_c < 1700 \text{ MeV}$. At such large momenta, the description of the kaon–nucleon interaction in terms of potentials becomes questionable. Furthermore, one should include momentum dependent terms in the kaon self-energy, which were not considered in Ref. [8]. A more realistic modification of the self-energy could push the critical momentum k_c to even larger values. Below, we argue that this, indeed, happens in the framework of a more constrained description of the K^- self-energy.

As was pointed in Ref. [2] the K^- spectrum shows a second branch related to the correlated $\Lambda(1116)$ particle and proton hole states with the quantum numbers of K^- mesons. The typical energy of this mode is $\omega \sim m_\Lambda - m_N \simeq 200 \text{ MeV}$. This low-lying branch is expected to manifest itself in neutron stars through a condensation of negative kaons with the finite momentum (p-wave condensation) [2] and in nucleus–nucleus collisions through an enhanced population of K^- modes, cf. Ref. [5].

On the low-lying branch in the K^- spectrum the condition $\omega < k$ is fulfilled at rather moderate kaon momenta ($k_c \simeq 200 \text{ MeV}$). Therefore, it is reasonable to apply the idea of R.F. Sawyer to a new energy–momentum domain nearby this branch. In this low-energy region K^- mesons are strongly coupled with hyperons. To constrain the K^- spectral density in nuclear matter from anti-neutrino nucleus scattering it is, therefore, necessary to consider other channels with strangeness production in the form of a hyperon $\bar{\nu}_l + N \rightarrow H + l^+$, where N stands for a nucleon and H is the corresponding hyperon, Λ or Σ . We shall show that these reaction channels give in fact a much larger contribution to the l^+ cross section as compared with the reaction channel with K^- production.

In dense matter one has to consider in-medium renormalization of the kaon and nucleon–hyperon weak currents. This renormalization due to short-range hyperon–nucleon correlations enhances substantially the coupling of in-medium kaons to the lepton weak current and suppresses the nucleon–hyperon weak current.

Due to the strong coupling of kaons to the Λ –proton-hole states, the K^- excitations are damped in matter. Therefore, a naive treatment of Feynman diagrams for reaction

above, drawn with the full in-medium propagators and vertices leads to double counting. A similar problem with in-medium pion has been discussed and resolved in Ref. [9,10], with the help of the optical theorem formalism [10]. In the present work, we apply this formalism to discriminate various processes with strangeness production. Following Refs [10,11], we express the strangeness production rates in terms of closed diagrams constructed with non-equilibrium Green's functions.

Finally, we calculate cross-sections of the neutrino induced strangeness production, utilizing the in-medium kaon spectral density, the short range $\Lambda - p$ correlations, and taking into account the in-medium vertex renormalization. Since a neutrino can easily pass through a nucleus and the path lengths of produced K^- mesons and Λ particles are rather small (at typical transverse momenta under consideration), finite-size effects can be neglected. We discuss the possibility to observe these processes in experiment, testing, thereby, strange degrees of freedom, in particular the kaon spectral density, in nuclear matter.

II. KAON SELF-ENERGY.

Let us begin with a discussion of kaon properties in cold nuclear matter, i.e., with the density $\rho = \rho_0 = 0.17 \text{ fm}^{-3}$ and the proton concentration $x = \rho_p/\rho = 1/2$. The Green's function of the K^- meson, D_{K^-} , is the solution of the Dyson equation,

$$\text{thick wavy line} = \text{thin wavy line} + \text{thin wavy line} \boxed{\Pi_{K^-}} \text{thick wavy line}, \quad (1)$$

where the thin wavy line is the Green's function of a free kaon. The thick wavy line is the full kaon propagator in medium, which in the momentum representation reads $D_{K^-}(\omega, k) = [\omega^2 - k^2 - m_K^2 - \Pi_{K^-}(\omega, k, \rho, x) + i0]^{-1}$. The frequency and the momentum of a kaon are denoted by ω and k , respectively. The notation m_K stands for the free kaon mass, and Π_{K^-} is the K^- self-energy. The latter contains several pieces related to the most important processes, $\Pi_{K^-} = \Pi_S + \Pi_P + \Pi_{\text{res}}$. The first term, Π_S , is the s-wave part of the K^- self-energy, generated by the s-wave kaon–nucleon scattering essential nearby the KN threshold [1,2,12]. The difference between various approaches with respect to the s-wave KN interaction is reflected mainly in the description of the energy–momentum region nearby the kaon branch of the spectrum. However, for parameterizations [12] considered, at present, as rather realistic, the kaon branch lies above the line $\omega = k$ up to very high kaon momenta $k_c \sim 2000 \text{ MeV}$. Therefore, we avoid a detailed discussion of uncertainties in Π_S term and, following Ref. [1], utilize it in a much more simple form $\Pi_S = -d m_K^2 \rho/\rho_0 - \alpha m_K \omega \rho/\rho_0$, with parameters $d \approx 0.18$ and $\alpha \approx 0.23$ taken from Refs. [2,5]. Further we intend to focus on another term of the kaon self-energy, which is responsible for the spectral density of the K^- states below line $\omega = k$.

The p-wave part of the K^- polarization operator is mainly determined by the contributions from the $\Lambda(1116)$ –proton-hole states and the $\Sigma(1193)$ –nucleon-hole intermediate states $\Pi_P = \Pi_\Lambda + \Pi_\Sigma$. In Ref. [2] it is argued that due to smallness of the kaon–nucleon– Σ coupling constant compared to the kaon–nucleon– Λ coupling constant ($C_{KN\Sigma}/C_{KN\Lambda} \simeq 0.2$) the contribution of Σ particles to the polarization operator is small. Therefore, we do not

consider small contributions of Σ hyperons, which structure is quite analogous to that of the Λ hyperon, and drop the term Π_Σ in the polarization operator.

The main contribution, Π_Λ , is depicted by the loop diagram

$$\Pi_\Lambda = \text{loop diagram} = -i C_{K N \Lambda} \int \frac{d^4 p}{(2\pi)^4} \tilde{C}_{K N \Lambda} \text{Tr} \left\{ \hat{k} \gamma_5 \hat{G}_\Lambda(p+k) \hat{k} \gamma_5 \hat{G}_N(p) \right\}, \quad (2)$$

where $\hat{G}_\alpha(p) = (\hat{p} + m_\alpha^*) G_\alpha(p) = (\hat{p} + m_\alpha^*) \{ [p^2 - m_\alpha^{*2} + i0]^{-1} + 2\pi i n_\alpha(p) \delta(p^2 - m_\alpha^{*2}) \}$ is the Green's function of a given baryon, $\alpha = p, \Lambda$; m_α^* is the in-medium mass of the baryon α taken according to Ref. [3], and n_α stands for the Fermi occupation factor of protons. The bare coupling constant is $C_{K N \Lambda} \simeq -1 m_\pi^{-1}$. Here and below, evaluating integrals with the Green's functions we drop the divergent medium-independent part, which is assumed to be contained in the physical values of particle masses and coupling constants. The fat blob in the diagram corresponds to the full $K N \Lambda$ vertex $\tilde{C}_{K N \Lambda}$, which takes into account baryon-baryon correlations. It is depicted by the following diagrams

$$\tilde{C}_{K N \Lambda} = \text{fat blob} = \text{blob} + \text{blob with loop} . \quad (3)$$

The shaded square represents the short-range Λ -proton interaction that can be written in the non-relativistic Landau-Migdal parameterization as

$$\text{shaded square} = T_{\Lambda p}^{\text{loc}} = C_{K N \Lambda}^2 [f_\Lambda + f'_\Lambda (\vec{\sigma}_\Lambda \vec{\sigma}_p)], \quad (4)$$

where σ_Λ and σ_p are the Pauli spin matrices of a Λ particle and a proton, respectively, f_Λ and f'_Λ are the Landau-Migdal parameters of the Λ - p interaction. This interaction is irreducible with respect to the hyperon-nucleon-hole intermediate states. The formal solution of Eq. (3) with the interaction (4) is given by

$$\tilde{C}_{K N \Lambda} = \gamma(f'_\Lambda) C_{K N \Lambda} = [1 - f'_\Lambda C_{K N \Lambda}^2 A_{p\Lambda}(\omega, k)]^{-1} C_{K N \Lambda} \quad (5)$$

with the loop integral $A_{p\Lambda}(\omega, k) = -i 8 m_N^{*2} \int \frac{d^4 p}{(2\pi)^4} G_\Lambda(p+k) G_N(p)$. We see that only the spin parameter f'_Λ enters expression (5). The empirical value of f'_Λ is not known. It could be, in principle, extracted from the data on multi-strange hypernuclei. For our purpose in this note we are contented with a rough estimation of this parameter. Following Ref. [13], we suggest that the hyperon-nucleon interaction is determined mainly by the kaon and K^* exchanges corrected by the short-range NN correlations

$$f'_\Lambda \simeq \frac{1}{3} \frac{m_0^2}{m_K^2 + m_0^2} + \frac{2}{3} \frac{C_{K^* N \Lambda}^2}{C_{K N \Lambda}^2} \frac{m_0^2}{m_{K^*}^2 + m_0^2}. \quad (6)$$

Here m_{K^*} denotes the mass of the heavy strange vector meson and m_0 is related to the inverse core radius of nucleon–nucleon interaction, i.e., $m_0 \simeq m_\omega$, being the mass of the ω meson. Utilizing the coupling constant of $K^*N\Lambda$ interactions, taken from the Jülich model of hyperon–nucleon interaction via the meson exchange, $C_{K^*N\Lambda} \simeq 1.74/m_\pi$, we estimate $f'_\Lambda \approx 1.1$. The calculations below will be done for two values of this parameter $f'_\Lambda = 0$ and $f'_\Lambda = 1.1$.

The last term of the self-energy, Π_{res} , includes residual interaction, which cannot be constrained from experiments with on-shell kaons. Therefore, its value and structure is rather ambiguous. In Refs [14,2] the residual off-shell interaction is suggested to be reconstructed with the help of low-energy theorems. These constrains, following from the current algebra and the PCAC hypothesis, can be safely applied in our present consideration, since the neutrino induced reaction probe directly the axial current correlator, for which the low-energy theorems have actually been formulated. Following Ref. [2], we cast the term Π_{res} as $\Pi_{\text{res}} = \lambda(m_{K^*}^2 - \omega^2 + k^2) \rho/\rho_0$ with the parameter $\lambda = 2d$. Without regard to the low-energy theorems one would put $\Pi_{\text{res}} = 0$.

Please note that the particular details of the kaon–nucleon interaction nearby the mass-shell (that can be found elsewhere [1,2,12]) do not affect qualitatively the description of kaon behavior at somewhat lower energies, which determine our discussion below. The crucial point for us is that a kaon couples to Λ -particle–hole states and propagates, thereby, in a frequency–momentum region not accessible for vacuum kaons. This coupling enforces K^- and Λ degrees of freedom to be treated consistently. We are rather going to discuss experimental consequences of a kaon modification, using the above formulated kaon self-energy for illustration and the short-range Λp interaction (4).

III. K^- SPECTRAL DENSITY.

The spectral density of kaon excitations is defined as $A_{K^-}(\omega, k) = -2\text{Im} D_{K^-}^R(\omega, k)$, where $D_{K^-}^R$ is the retarded Green's function of the K^- meson. The left panel in Fig. 1 shows the contour plot of $A_{K^-}(\omega, k)$ calculated for $\rho = \rho_0$ and $x = 1/2$. The upper solid line corresponds to the quasiparticle kaon branch. In the framework of our simplified treatment of the s-wave K^-N interaction the spectral density is a δ -function, $A_{K^-}(\omega, k) = [\tilde{\Gamma}_{K^-}(k)/2\omega_{K^-}(k)] \delta(\omega - \omega_{K^-}(k))$ for ω nearby $\omega_{K^-}(k)$, where $\omega_{K^-}(k)$ is the solution of the dispersion equation $\text{Re}[D_{K^-}^R(\omega, k)]^{-1} = 0$, which determines the kaon branch of the spectrum. The factor $\tilde{\Gamma}_{K^-}(k) = 2\omega_{K^-}(k) [\partial \text{Re} D_{K^-}^R(\omega_{K^-}(k), k)/\partial \omega]^{-1}$ measures how strongly the kaon branch is populated by the in-medium K^- mesons, cf. Ref. [2]. It indicates the relative weight of this branch in the full spectral density. The dot-dashed line on the left panel in Fig. 1 is the upper border of the region $\omega < k$, where the processes under consideration may occur. We see that the upper quasiparticle kaon branch does not cross this border for momenta $k < k_c$, where the critical momentum $k_c = m_K(1 - d + \lambda)/\alpha \approx 2570$ MeV (for $\lambda = 2d$ that corresponds to the more constrained description) and $k_c \approx 1570$ MeV (for $\lambda = 0$, i.e., when one ignores constrains of the low-energy theorems).

Below the kaon branch in Fig. 1 are shown the contour lines of the kaon spectral density in the Λ -proton-hole continuum. The latter is bordered by the dashed lines. Within the continuum the imaginary part of the kaon propagator is non-zero, $\text{Im} \Pi_\Lambda \neq 0$, that corre-

sponds to processes $K^- \leftrightarrow \Lambda + p^{-1}$ (p^{-1} means the proton hole). The relative strength of this region in the spectral density is characterized by the quantity

$$\tilde{\Gamma}_\Lambda(k) = \int_{\omega_{p\Lambda}^-(k)}^{\omega_{p\Lambda}^+(k)} \frac{d\omega}{2\pi} 2\omega A_{K^-}(\omega, k), \quad (7)$$

where $\omega_{p\Lambda}^\pm(k)$ is the upper (+) and lower (−) borders of Λp^{-1} continuum,

$$\omega_{p\Lambda}^+(k) = \begin{cases} \sqrt{(m_\Lambda^* - m_N^*)^2 + k^2} & , \quad k < p_{pF} (m_\Lambda^* - m_N^*)/m_N^* \\ \sqrt{m_\Lambda^{*2} + (k + p_{pF})^2} - \sqrt{m_N^{*2} + p_{pF}^2} & , \quad k > p_{pF} (m_\Lambda^* - m_N^*)/m_N^* \end{cases},$$

$$\omega_{p\Lambda}^-(k) = \sqrt{m_\Lambda^{*2} + (k - p_{pF})^2} - \sqrt{m_N^{*2} + p_{pF}^2},$$

p_{pF} stands for the Fermi momentum of the protons. The values of the occupation factors $\tilde{\Gamma}_{K^-}(k)$ and $\tilde{\Gamma}_\Lambda(k)$ are shown in the right panel of Fig. 1. We observe that the main weight is carried by the kaon branch, whereas the lower Λp^{-1} continuum is populated by K^- only on a percentage level.

Please notice that in the quasiparticle limit, $\text{Im}\Pi \rightarrow 0$, our kaon spectrum has only one kaon branch and the dispersion equation $\text{Re}[D_{K^-}^R(\omega, k)]^{-1} = 0$ has no low-energy solution. Only in the resonance approximation for the real part of the particle–hole loop such a solution exists, cf. [2]. In this case one can approximately treat the low-energy region as a quasiparticle branch. Besides, with taking into account the complicated threshold dynamics in K^-N scattering nearby threshold, leading to the dynamical $\Lambda^*(1405)$ resonance, the upper quasiparticle kaon branch becomes also a region of the spectral density. Hence, in reality, we discuss experimental manifestation of the regions on the frequency–momentum plane, where the spectral function does not vanish, rather than manifestation of quasiparticle branches. For brevity’s sake we continue to speak about “the branches”, bearing in mind regions of particle–hole continua populated by mesonic excitations.

The description of the kaon–nucleon interaction formulated above (cf. Ref. [2]) is quite analogous to that well known from pion–nucleon physics, cf. [15]. Except for a spin and an isospin, hyperons play the same role in kaon physics, as Δ isobars do in pion physics. The crucial difference, however, is that the corresponding Δ branch in the pion spectrum lies above the pion branch, whereas the Σ and Λ branches of the K^- spectrum lie below the kaon branch. The difference in the description of the s-wave interactions in the pion and the kaon cases arises mainly due to distinct values of the corresponding Σ -terms. The pion–nucleon Σ -term is much smaller than the kaon–nucleon one. Due to this, pion condensation may occur at sufficiently high density $\rho \gtrsim 2\rho_0$ due to attractive p-wave interaction, as has been suggested by A.B. Migdal, R.F. Sawyer, and D.J. Scalapino, cf. Ref. [16]. On the contrary, kaon condensation may occur as due to the s-wave attraction [1] as due to the p-wave one [2] (the latter possibility is analogous to that in the pion case). The choice between these possibilities depends on the interplay between strengths of not well known s- and p-wave interactions in dense nuclear matter.

The neutrino reactions discussed in this paper might give an extra important information on strange particle interaction in nuclear matter. It could yield additional constrains on the K^- – Λ –nucleon interaction.

IV. WEAK INTERACTION IN MEDIUM

The kaon decay processes in vacuum are determined by the current $J_K^\mu = i\sqrt{2}f_K k^\mu$, where f_K stands for the kaon decay constant. In the nuclear medium this current is modified due to strong interaction, $\tilde{J}_K^\mu = i\sqrt{2}f_K \Gamma^\mu(k)$, where the vertex function $\Gamma(k)$ is mainly determined by the following diagrams

$$\text{Diagram (8)} \quad (8)$$

Here the small diamond symbolizes the bare coupling of kaonic and leptonic currents, the small box represents the matrix element of the weak hadronic current between Λ and proton-hole states $W_S^\mu = -\gamma^\mu (g_V^S + g_A^S \gamma_5)$, the vector coupling constant is $g_V^S = \sqrt{\frac{3}{2}}$ and the axial coupling constant is $g_A^S \approx 0.62\sqrt{\frac{3}{2}}$. The Λp interaction in the intermediate states given by Eq. (4) is absorbed into the dressed vertex of KNA interaction depicted by the fat circle. The dashed lines symbolize an attached leptonic weak current. From Eq. (8) we get

$$\begin{aligned} \sqrt{2}f_K \Gamma^\mu &= \sqrt{2}f_K k^\mu - \frac{g_A^S}{C_{KNA}} P_A^\mu, \\ P_A^\mu &= i C_{KNA} \tilde{C}_{KNA} \int \frac{d^4 p}{(2\pi)^4} \text{Tr} \left\{ \hat{k} \gamma_5 \hat{G}_\Lambda(p+k) \gamma^\mu \gamma_5 \hat{G}_N(p) \right\}. \end{aligned} \quad (9)$$

Taking into account that $(P_A \cdot k) = \Pi_\Lambda^-$, cf. Eq. (2), we obtain

$$\begin{aligned} \Gamma^\mu &= k^\mu \left(1 - \frac{A}{\vec{k}^2} \right) - \frac{\delta^{\mu 0}}{k^2} B, \\ A(\omega, \vec{k}) &= \Delta_S \left[\omega P_A^0(\omega, \vec{k}) - \Pi_\Lambda^-(\omega, \vec{k}) \right], \\ B(\omega, \vec{k}) &= -\omega A(\omega, \vec{k}) + \vec{k}^2 \Delta_S P_A^0(\omega, \vec{k}), \end{aligned} \quad (10)$$

where $\Delta_S = g_A^S / (\sqrt{2} C_{KNA} f_K)$ is the discrepancy of the Goldberger–Treiman relation, which is about 67%.

We will also consider reactions with the leptonic current directly attached to the nucleon–hyperon weak current. In this case, we have to take into account the modification of the latter due to the short-range correlation of nucleons and hyperons. We determine the in-medium Λ – p weak current, \tilde{W}_S^μ , by the following diagram equation

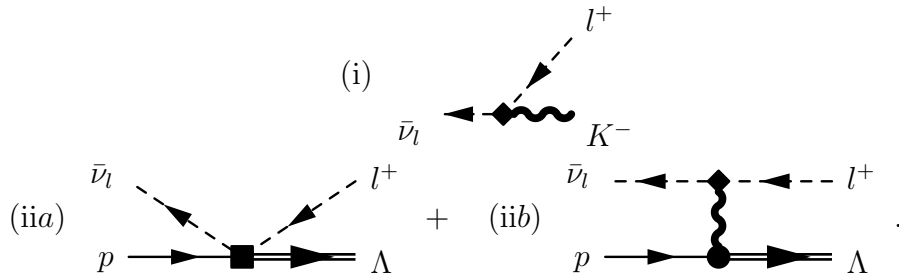
$$\tilde{W}_S^\mu = \text{Diagram (11)} \quad (11)$$

This current \tilde{W}_S^μ is irreducible with respect to one-kaon exchange. The solution of Eq. (11) with the interaction (4) reads $\tilde{W}_S^\mu = -\gamma^\mu [\gamma_\Lambda(f_\Lambda) g_V^S + \gamma_\Lambda(f'_\Lambda) g_A^S \gamma_5]$, where the function γ_Λ is given by Eq. (5).

Provided with both weak interactions (8) and (11), and with the kaon propagator in medium, we are able to consider the neutrino induced reactions with associated $S = -1$ strangeness production.

V. ANTI-NEUTRINO SCATTERING WITH STRANGENESS PRODUCTION.

The negative strangeness in a nucleus can be produced by neutrino via the following reactions: (i) the neutrino decay $\bar{\nu}_l \rightarrow l^+ + K^-$ and (ii) the Λ production on a nucleon $\bar{\nu}_l + p \rightarrow l^+ + \Lambda$. Other processes with more particles in the initial and final states give smaller contribution since their phase space volume is suppressed. As in vacuum one may depict the processes (i)–(ii) by the following diagrams



Taking into account in-medium effects, however, one uses the thick wavy line for the in-medium K^- meson and the fat vertices to indicate in-medium renormalization given by Eqs (3), (8) and (11).

Proceeding naively, one would calculate the amplitude of strangeness production as the sum of the squared matrix elements of reaction (i) and (ii), summing two contributions in (ii) coherently. We show that this approach will immediately lead to double counting.

Let us consider, first, the reaction (i), proposed by R.F. Sawyer to test the kaon spectrum in medium. Utilizing the modified kaon weak current we present the matrix element of the process $\bar{\nu}_l \rightarrow K^- + l^+$ as

$$\mathcal{M}_{K^-} = i G f_K \sin \theta_C (\Gamma(k) \cdot l).$$

Here, G stands for the Fermi constant of the weak interaction, θ_C denotes the Cabbibo angle, and $l_\mu = \bar{u}_\nu \gamma_\mu (1 - \gamma_5) u_l$ is the leptonic current. Carrying out summation of the squared matrix element over the lepton spin and averaging over the neutrino spin we obtain

$$V_{K^-}(E_\nu, \omega, \vec{k}) = \frac{1}{2} \sum_{\text{spin}} |\mathcal{M}_{K^-}|^2 = \frac{1}{2} G^2 f_K^2 \sin^2 \theta_C \Gamma^\alpha(k) \Gamma^{\dagger\beta}(k) \sum_{\text{spin}} l_\alpha l_\beta^\dagger.$$

The summation over spins gives

$$L^{\alpha\beta} = \sum_{\text{spin}} l^\alpha l^{\dagger\beta} = 8 \left[p_l^\alpha p_\nu^\beta + p_l^\beta p_\nu^\alpha - g^{\alpha\beta} (p_l \cdot p_\nu) - i \varepsilon^{\alpha\beta\gamma\delta} p_{l\gamma} p_{\nu\delta} \right], \quad (12)$$

and we find

$$V_{K^-}(E_\nu, \omega, \vec{k}) = -4 G^2 f_K^2 \sin^2 \theta_C \left[m_l^2 F_1(\omega, \vec{k}) - 2 F_2(\omega, \vec{k}, E_\nu) \right], \quad (13)$$

where

$$F_1(\omega, \vec{k}) = \left\{ \left| \omega - \frac{\omega A + B}{\vec{k}^2} \right|^2 - \vec{k}^2 \left| 1 - \frac{A}{\vec{k}^2} \right|^2 \right\},$$

$$F_2(\omega, \vec{k}, E) = \frac{|B|^2}{\vec{k}^4} \left\{ \left(E - \frac{1}{2} \omega \right)^2 - \frac{1}{4} \vec{k}^2 \right\}.$$

The differential production rate renders, then,

$$\frac{d\mathcal{W}_l^{(i)}}{dE_l dx dt} = \frac{\sqrt{E_l^2 - m_l^2}}{16 \pi^2 E_\nu} \left[-2 \text{Im} D_{K^-}^R(\bar{\omega}_l, \bar{k}_l) \right] V_{K^-}(E_\nu, \bar{\omega}_l, \bar{k}_l). \quad (14)$$

Here $\bar{\omega}_l = E_\nu - E_l$ is the kaon frequency for the process with a given lepton in the final states $l = e^+, \mu^+$, and $\bar{k}_l = \sqrt{E_\nu^2 + E_l^2 - m_l^2 - 2 x_l E_\nu \sqrt{E_l^2 - m_l^2}}$ is the corresponding kaon momentum, where $x_l = \cos \theta_l$ for θ_l , being the angle between an incoming anti-neutrino and an outgoing lepton. Considering the nucleus with a weight A to be a uniform sphere of the radius $R = r_0 A^{1/3}$ (where $r_0 \simeq 1.2$ fm), we present the differential cross section of the positive lepton production as

$$\frac{d\sigma_l^{(i)}}{dE_l dx} = 2 \pi r_0^3 A \frac{d\mathcal{W}_l^{(i)}}{dE_l dx dt}. \quad (15)$$

In Fig. 2 we show the differential cross sections per A of the e^+ (left panel) and μ^+ (right panel) production by a neutrino with energy $E_\nu = 1$ GeV. We observe that the cross sections are strongly peaked as the function of lepton energy for small lepton scattering angles, $x > 0.95$. At larger angles $0.8 < x < 0.95$, the cross sections decrease rapidly by factor 5 for e^+ and 3 for μ^+ , and are shifted to smaller lepton energies. At angles corresponding to $x < 0.8$, the positron production cross section decreases further and becomes almost negligible, whereas for positive muons the cross section decreases moderately. Due to this, the angular integrated cross section of muons is larger than that of positrons, especially at smaller lepton energies. Having integrated over the lepton energy, we obtain for the total cross sections of the $e^+(\mu^+)$ production

$$A^{-1} \sigma(\bar{\nu}_e \rightarrow K^- + e^+) \approx 1 \times 10^{-42} \text{ cm}^2, \quad A^{-1} \sigma(\bar{\nu}_\mu \rightarrow K^- + \mu^+) \approx 4 \times 10^{-42} \text{ cm}^2.$$

We note that the μ^+ production cross section is larger than positron one by factor ≈ 4 , only. This is in contrast to expectation based upon the vacuum branching ratios of a kaon decay $\Gamma(K^- \rightarrow e^- + \nu_e)/\Gamma(K^- \rightarrow \mu^- + \nu_\mu) \approx 2.5 \times 10^{-5}$. For the bare weak interaction the squared matrix element of the reaction $\bar{\nu}_l \rightarrow K^- + l^+$ would be $|\mathcal{M}|^2 \propto m_l^2 [m_l^2 - (k \cdot k)]/2$, that explains a strong enhancement of muon processes in vacuum compared with the positron ones. In medium the weak kaon current is dramatically modified due to the mixture of kaons with the Λ -particles–proton hole states carrying the same quantum numbers, see the second diagram in Eq. (8). As the result, the squared matrix element of the reaction (13) does not possess strong dependence on the lepton mass. Therefore, in medium squared matrix elements for positrons and muons turn out to be of the same order of magnitude.

Please notice that the process considered here, following the arguments of R.F. Sawyer, probes the kaon spectral density in the whole frequency–momentum region rather than nearby the kaon branch as it was considered in Ref. [8]. Indeed, the K^- spectral density in Eq. (14) can be split as following

$$-2\text{Im} D_{K^-}^R(\omega, k) = 2\text{Im} \Pi_\Lambda(\omega, k) |D_{K^-}^R(\omega, k)|^2 + 2\delta\text{Im} \Pi_{K^-}(\omega, k) |D_{K^-}^R(\omega, k)|^2. \quad (16)$$

The first term in the decomposition (16) corresponds to the low-energy kaonic states in the Λ –proton-hole continuum, whereas the second one is related to the contribution of other kaon dissipation processes. In our approximation for the s-wave KN interaction the residual part of the spectral density is δ -function-like

$$2\delta\text{Im} \Pi_{K^-}(\omega, k) |D_{K^-}^R(\omega, k)|^2 = 2\pi \delta(\omega^2 - k^2 - m_K^2 - \text{Re} \Pi_{K^-}(\omega, k)) \theta(\omega - \omega_{p\Lambda}^+(k)), \quad (17)$$

where $\theta(x)$ is the Heaviside's step function. In Ref. [8] only the second term in Eq. (16) was considered, in which the δ function was smoothed by a constant width. In our case this term starts to contribute only when the kaon momentum exceeds the critical value k_c , which is the solution of the equation $m_K^2 + \text{Re} \Pi_{K^-}(\omega = k_c, |\vec{k}| = k_c) = 0$. For our polarization operator, constrained by the low-energy theorems, the value $k_c = 2570$ MeV is substantially larger than that (~ 1600 MeV) obtained in Ref. [8]. (We recover the latter value putting $\lambda = 0$.) Therefore, it seems that the region of the kaon spectral density considered in Ref. [8] is unlikely to be probed by anti-neutrinos with energies less than the threshold value $E_\nu^{\text{thr}} \simeq 2570$ MeV.

On the other hand, we have seen that the first term in the kaon spectral density contributes at much smaller neutrino energies. However, in this case we deal with the kaon which, being produced, decays into the Λ particle and the proton-hole, i.e., this process occurs exactly in the same neutrino-energy region, where the process $\bar{\nu}_l + p \rightarrow \Lambda + l^+$ does. This invites us to investigate the probability of the latter in more detail.

According to the diagrams (ii) above, the matrix element of the reaction $\bar{\nu}_l + p \rightarrow \Lambda + l^+$ can be written as

$$\mathcal{M}_\Lambda^{(\text{ii})} = \mathcal{M}_\Lambda^{(\text{ii}a)} + \mathcal{M}_\Lambda^{(\text{ii}b)} = \frac{1}{\sqrt{2}} G \sin \theta_C l_\mu \bar{u}_\Lambda (\widetilde{W}_S^\mu + \sqrt{2} f_K \widetilde{C}_{KN\Lambda} \Gamma^\mu \hat{k} \gamma_5 D_{K^-}) u_p.$$

For the squared, spin averaged matrix element we obtain

$$\frac{1}{2} \sum_{\text{spin}} |\mathcal{M}_\Lambda|^2 = \frac{1}{2} \sum_{\text{spin}} |\mathcal{M}_\Lambda^{(\text{ii}a)}|^2 + \frac{1}{2} \sum_{\text{spin}} 2 \text{Re} \left\{ \mathcal{M}_\Lambda^{(\text{ii}b)} \mathcal{M}_\Lambda^{\dagger(\text{ii}a)} \right\} + \frac{1}{2} \sum_{\text{spin}} |\mathcal{M}_\Lambda^{(\text{ii}b)}|^2 \quad (18)$$

with

$$\frac{1}{2} \sum_{\text{spin}} |\mathcal{M}_\Lambda^{(\text{ii}a)}|^2 = \frac{1}{2} G^2 \sin^2 \theta_C \text{Tr} \left\{ \widetilde{W}_S^\mu (\hat{p}_\Lambda + m_\Lambda^*) \widetilde{W}_S^{\dagger\nu} (\hat{p}_p + m_N^*) \right\} L_{\mu\nu}, \quad (19)$$

$$\frac{1}{2} \sum_{\text{spin}} 2 \text{Re} \left\{ \mathcal{M}_\Lambda^{(\text{ii}b)} \mathcal{M}_\Lambda^{\dagger(\text{ii}a)} \right\} = G^2 \sin^2 \theta_C f_K$$

$$\times 2 \operatorname{Re} \left[\tilde{C}_{KN\Lambda}^\dagger D_{K^-}^{R\dagger} \Gamma^{\dagger\mu} \operatorname{Tr} \left\{ \hat{k} \gamma_5 (\hat{p}_\Lambda + m_\Lambda^*) \widetilde{W}_S^\nu (\hat{p}_p + m_N^*) \right\} \right] L_{\mu\nu}, \quad (20)$$

$$\frac{1}{2} \sum_{\text{spin}} |\mathcal{M}_\Lambda^{(\text{ii}b)}|^2 = V_{K^-}(E_\nu, \omega, k) |\tilde{C}_{KN\Lambda}|^2 |D_{K^-}^R|^2 \operatorname{Tr} \left\{ \hat{k} \gamma_5 (\hat{p}_\Lambda + m_\Lambda^*) \hat{k} \gamma_5 (\hat{p}_p + m_N^*) \right\}. \quad (21)$$

Here $L_{\mu\nu}$ is the leptonic tensor (12), and p_Λ and p_p are momenta of the Λ particle and the proton, respectively. Utilizing kinematics of the reaction, the first term in Eq. (18) renders

$$\begin{aligned} \frac{1}{2} \sum_{\text{spin}} |\mathcal{M}_\Lambda^{(\text{ii}a)}|^2 &= V_\Lambda((p_p \cdot p_\nu), \omega, \vec{k}) \\ &= G^2 \sin^2 \theta_C \left\{ 4 [(k \cdot k) - \Delta] [(k \cdot k) - m_l^2] \right. \\ &\quad \times \left[(g_V^S)^2 |\gamma_\Lambda(f_\Lambda)|^2 - g_A^S g_V^S \operatorname{Re} [\gamma_\Lambda(f_\Lambda) \gamma_\Lambda^\dagger(f'_\Lambda)] + (g_A^S)^2 |\gamma_\Lambda(f'_\Lambda)|^2 \right] \\ &\quad + 16 \left[(g_V^S)^2 |\gamma_\Lambda(f_\Lambda)|^2 + (g_A^S)^2 |\gamma_\Lambda(f'_\Lambda)|^2 \right] \\ &\quad \times \left(2 (p_p \cdot p_\nu)^2 + (p_p \cdot p_\nu) [(k \cdot k) - \Delta - m_l^2] \right) \\ &\quad - 16 g_A^S g_V^S \operatorname{Re} [\gamma_\Lambda(f_\Lambda) \gamma_\Lambda^\dagger(f'_\Lambda)] (p_p \cdot p_\nu) (k \cdot k) \\ &\quad \left. + 8 \left[(g_V^S)^2 |\gamma_\Lambda(f_\Lambda)|^2 - (g_A^S)^2 |\gamma_\Lambda(f'_\Lambda)|^2 \right] m_N^* m_\Lambda^* [m_l^2 - (k \cdot k)] \right\}, \quad (22) \end{aligned}$$

where $(k \cdot k) = \omega^2 - \vec{k}^2$, $\Delta = m_\Lambda^{*2} - m_N^{*2}$, and p_ν and p_p are momenta of an anti-neutrino and a proton, respectively. In Eqs (20) and (21) we recognize the traces appearing in Eqs. (9) and (2), that allow us to calculate them with ease.

After integrating over the phase-space volume we obtain the differential rate of the reaction $\bar{\nu}_l + p \rightarrow \Lambda + l^+$ as

$$\frac{d\mathcal{W}_l^{(\text{ii})}}{dE_l dx dt} = \frac{d\mathcal{W}_l^{(\text{ii}a)}}{dE_l dx dt} + \frac{d\mathcal{W}_l^{(\text{ii}ab)}}{dE_l dx dt} + \frac{d\mathcal{W}_l^{(\text{ii}b)}}{dE_l dx dt}. \quad (23)$$

Three terms here are the contributions from diagram (ii a), interference term between diagrams (ii a) and (ii b), and diagram (ii b), respectively. The first term yields

$$\frac{d\mathcal{W}_l^{(\text{ii}a)}}{dE_l dx dt} = \frac{\sqrt{E_l^2 - m_l^2}}{16 \pi^2 E_\nu} 2 \operatorname{Im} \left[(-i) \int \frac{d^4 p}{(2\pi)^4} G_N(p) G_\Lambda(p + \bar{k}_l) V_\Lambda((p_\nu \cdot p), \bar{\omega}_l, \bar{k}_l) \right], \quad (24)$$

where the frequency $\bar{\omega}_l$ and the momentum \bar{k}_l are defined as in Eq. (14). In the second term we use $\Delta_S \operatorname{Im} P_A^\mu = -\operatorname{Im} \Gamma^\mu$ and separate explicitly the real and imaginary parts of the kaon propagator. Then, the second term reads

$$\begin{aligned} \frac{d\mathcal{W}_l^{(\text{ii}ab)}}{dE_l dx dt} &= \frac{\sqrt{E_l^2 - m_l^2}}{16 \pi^2 E_\nu} \left\{ 2 \operatorname{Re} D_{K^-}^R(\bar{\omega}_l, \bar{k}_l) V_K^{(1)}(E_\nu, \bar{\omega}_l, \bar{k}_l) \right. \\ &\quad \left. - 2 \operatorname{Im} D_{K^-}^R(\bar{\omega}_l, \bar{k}_k) V_K^{(2)}(E_\nu, \bar{\omega}_l, \bar{k}_l) \right\}, \quad (25) \end{aligned}$$

where

$$\begin{aligned} V_K^{(1)}(E_\nu, \omega, k) &= 2 G^2 \sin^2 \theta_C f_K^2 (\text{Re } \Gamma^\mu \text{Im } \Gamma^{\dagger\nu} L_{\mu\nu}), \\ V_K^{(2)}(E_\nu, \omega, k) &= 2 G^2 \sin^2 \theta_C f_K^2 (\text{Im } \Gamma^\mu \text{Im } \Gamma^{\dagger\nu} L_{\mu\nu}). \end{aligned}$$

The last term in Eq. (23) renders

$$\frac{d\mathcal{W}_l^{(\text{iib})}}{dE_l dx dt} = \frac{\sqrt{E_l^2 - m_l^2}}{16 \pi^2 E_\nu} \left[-2 \text{Im } \Pi_\Lambda(\bar{\omega}_l, \bar{k}_l) |D_{K^-}^R(\bar{\omega}_l, \bar{k}_l)|^2 \right] V_{K^-}(E_\nu, \omega, k). \quad (26)$$

Comparing this expression with Eqs (14) and (16) we observe that exactly the same term has been already taken into account in Eq. (14) with the first term of the kaon spectral density (16). This demonstrates the mentioned problem of double counting, which appears if one blindly includes medium effects in Feynman diagrams.

The differential cross section of the l^+ production in the reaction $\bar{\nu}_l + p \rightarrow \Lambda + l^+$ can be calculated using Eq. (15)

$$\frac{d\sigma_l^{(\text{ii})}}{dE_l dx} = 2 \pi r_0^3 A \left\{ \frac{d\mathcal{W}_l^{(\text{iiia})}}{dE_l dx dt} + \frac{d\mathcal{W}_l^{(\text{iiab})}}{dE_l dx dt} \right\}. \quad (27)$$

Here we dropped the term (26) included in our analysis of process (i).

Fig. 3 shows the results for the anti-neutrino energy of 1 GeV. We find that the difference between the positron and muon reactions is very small, therefore in Fig. 3 we show the result for positron production only. The solid and dashed lines are related to calculations without and with account for the in-medium renormalization of the weak interaction in process (iiia), i.e., in the first term in Eq. (27). To be specific, in our calculation we put $f_\Lambda = f'_\Lambda$. In Fig. 3 we see that the short-range ΛN correlations (factors γ_Λ in Eq. (22)) suppress the cross section of the reaction (iiia) and change the shape of the lepton spectrum.

The contribution from the interference terms between processes (iiia) and (iiib) is found to be very small and is not distinguishable on the scale of Fig. 3.

In Fig. 3 we observe that the positron production cross section decreases monotonically with the increasing positron scattering angle. The angular integrated cross section remains almost constant in a wide interval of the positron energy. The total cross section of the Λ production on a nucleus is

$$A^{-1} \sigma(\bar{\nu}_e + p \rightarrow e^+ + \Lambda) \approx A^{-1} \sigma(\bar{\nu}_\mu + p \rightarrow \mu^+ + \Lambda) \approx 2 \times 10^{-39} \text{ cm}^2.$$

In the total cross section the correlations result in a decrease of $\sim 10\%$.

As we can see, reaction $\bar{\nu}_l + p \rightarrow l^+ + \Lambda$ gives the main contribution to the strangeness production by anti-neutrino on a nucleus¹. Besides, this process occurs in the same kinematic

¹The cross sections in Fig. 2 and those of Ref. [8] are of the same order of magnitude despite the different energies used.

region as the reaction $\bar{\nu}_l \rightarrow l^+ + K^-$. Therefore, one needs more peculiar analysis, in order to separate the contribution of the K^- channel.

In principle, one can suggest to observe directly K^- mesons produced by an anti-neutrino on a nucleus. However, the kaons produced in reaction (i) are too far off mass-shell to lap from an in-medium state to a vacuum one. They have to gather the energy in the sequence of proceeding rescattering processes. Additionally free kaons can be produced in the two-step processes with a Λ decay, e.g., $\bar{\nu}_l + p \rightarrow l^+ + \Lambda \rightarrow l^+ + p + K^-$. This is a surface reaction, since the K^- has rather short mean free path in nuclear matter. Thereby, the yield of this reaction is suppressed. The similar process with a direct pion production has been considered in Ref. [17].

VI. OPTICAL-THEOREM FORMALISM FOR NEUTRINO SCATTERING

The example, considered above, demonstrates clearly that naive account of in-medium effects could lead to double counting. In the particular simplified case it was rather easy to resolve the problem. In general case, with account for more in-medium degrees of freedom coupled to the neutrino-lepton weak current, the double counting problem becomes very serious. Therefore, one needs an approach, within which such a problem does not exist or can be easily resolved. In Refs. [10,11] it was shown that the formalism of the optical theorem formulated in terms of non-equilibrium Green's functions allows to avoid the double counting problem.

Applying this approach to the anti-neutrino-nucleus scattering we can express the transition probability between the initial state with an anti-neutrino $\bar{\nu}_l$ and the final state with a positive lepton l^+ in terms of an evolution operator S as follows

$$\frac{d\mathcal{W}_{\bar{\nu} \rightarrow l^+}^{\text{tot}}}{dt} = \frac{dp_l^3}{(2\pi)^3 4 E_\nu E_l} \sum_{\{X\}} \overline{\langle \bar{\nu}_l | S^\dagger | l^+ + X \rangle \langle l^+ + X | S | \bar{\nu}_l \rangle}, \quad (28)$$

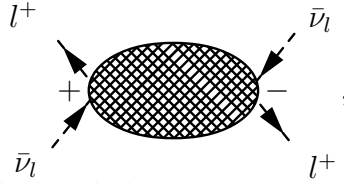
where we write explicitly the phase-space volume of initial ($\bar{\nu}_l$) and final (l^+) states. The bar denotes statistical averaging. The summation goes over complete set of all possible intermediate states $\{X\}$ constrained by the energy-momentum conservation law.

Making use of the smallness of the Fermi weak-interaction constant G , we can take into account processes in first order in G . Then, we expand the evolution operator S as

$$S \approx 1 - i \int_{-\infty}^{+\infty} T \{ V_W(x) S_{\text{nucl}}(x) \} dx_0, \quad (29)$$

where V_W is the Hamiltonian of the weak interaction, $V_W = \frac{G}{\sqrt{2}} l_\mu (W_S^\mu + J_K^\mu)$, taken in Eq. (29) in the interaction representation, and S_{nucl} is the part of the S matrix corresponding to the nuclear interaction, and $T\{\dots\}$ stands for the chronological ordering operator. After substitution of the S matrix (29) into Eq. (28) and averaging over the arbitrary non-equilibrium state of a nuclear system, there appear chronologically, anti-chronologically ordered exact Green's functions, denoted as G^{--} and G^{++} respectively, and disordered Green's functions G^{+-} and G^{-+} . The latter ones are related to Wigner's densities.

In graphical form the general expression for the probability of positive lepton production by an anti-neutrino is determined by the diagram



which represents the sum of all closed diagrams containing at least one $(+-)$ line. The contributions of specific processes contained in a closed diagram can be made visible by cutting the diagram over the $(+-)$, $(-+)$ lines, corresponding to exact G^{+-} and G^{-+} Green's functions.

The various contributions from $\{X\}$ can be classified according to global characteristics, such as strangeness, parity etc. Then, we can write, e.g.,

$$\begin{aligned} \frac{d\mathcal{W}_{\bar{\nu} \rightarrow l^+}^{\text{tot}}}{dt} &= \frac{d\mathcal{W}_{\bar{\nu} \rightarrow l^+}^{\Delta S=0}}{dt} + \frac{d\mathcal{W}_{\bar{\nu} \rightarrow l^+}^{\Delta S=-1}}{dt} + \dots \\ &= \frac{d^3 p_l}{(2\pi)^3 4 E_\nu E_l} \left(\begin{array}{c} l^+ \\ \nearrow \quad \searrow \\ + \quad \Delta S = 0 \quad - \\ \nwarrow \quad \nearrow \\ \bar{\nu}_l \end{array} + \begin{array}{c} l^+ \\ \nearrow \quad \searrow \\ + \quad \Delta S = -1 \quad - \\ \nwarrow \quad \nearrow \\ \bar{\nu}_l \end{array} \dots \right) . \quad (30) \end{aligned}$$

The first term represents all processes with the total strangeness 0 in the intermediate states. The second term contains the processes with the total strangeness -1 . Ellipses symbolize all other processes. In Ref. [10] it was shown that each blob in Eq. (30) can be considered as a propagation of some quanta of the in-medium interaction with certain quantum numbers. We illustrate it with the example of strangeness production, considered explicitly in the previous section.

A. Strange channel

Restricting our consideration to processes (iia) and (iib), we decompose the second blob in Eq. (30) as

$$\begin{array}{c} l^+ \\ \nearrow \quad \searrow \\ + \quad \Delta S = -1 \quad - \\ \nwarrow \quad \nearrow \\ \bar{\nu}_l \end{array} = \begin{array}{c} l^+ \\ \nearrow \quad \searrow \\ + \quad \dots \quad - \\ \nwarrow \quad \nearrow \\ \bar{\nu}_l \end{array} K^- + \begin{array}{c} l^+ \\ \nearrow \quad \searrow \\ + \quad \text{blob} \quad - \\ \nwarrow \quad \nearrow \\ \bar{\nu}_l \end{array} \dots \quad (31)$$

Ellipses symbolize other more complicated processes with more $(+-)$, $(-+)$ lines in the intermediate states, which within the Feynman diagram formalism would be depicted by the diagrams with more particles in initial and final states. The contributions of such processes are suppressed due to the smaller phase-space volume. By this reason we drop them.

The decomposition (31) is done according to the following principles: We separate two channels with strangeness exchange via a kaon (the first diagram) and a Λ -proton-hole (the second diagram). The kaon exchange in the first diagram has to be irreducible with respect to the Λ -proton-hole. Therefore, the dotted line symbolizes an in-medium kaon dressed by the s-wave and residual parts of the kaon polarization operator only. In diagrams it can be shown as follows

$$\dots\dots = \text{wavy} + \text{wavy} \boxed{\Pi_S} \dots\dots + \text{wavy} \boxed{\Pi_{\text{res}}} \dots\dots . \quad (32)$$

The shaded vertex in the second diagram in (31) is irreducible with respect to the $(+-)$ and $(-+)$ kaon line and the $(+-)$ and $(-+)$ Λ -proton-hole lines. This means it contains only the lines of a given sign, all $(--)$ or $(++)$. Thereupon, we drop this sign notation for the sake of brevity. Separating explicitly the Λ -particle-proton-hole states, we have

$$\begin{array}{c} l^+ \\ \swarrow \quad \searrow \\ \text{shaded vertex} \\ \swarrow \quad \searrow \\ \bar{\nu}_l \end{array} = \begin{array}{c} l^+ \\ \swarrow \quad \searrow \\ \text{triangle} \\ \swarrow \quad \searrow \\ \bar{\nu}_l \end{array} + \begin{array}{c} l^+ \\ \swarrow \quad \searrow \\ \text{loop} \\ \swarrow \quad \searrow \\ \bar{\nu}_l \end{array} , \quad (33)$$

where

$$\begin{array}{c} l^+ \\ \swarrow \quad \searrow \\ \text{triangle} \\ \swarrow \quad \searrow \\ \bar{\nu}_l \end{array} = \begin{array}{c} l^+ \\ \swarrow \quad \searrow \\ \text{dotted line} \\ \swarrow \quad \searrow \\ \bar{\nu}_l \end{array} + \begin{array}{c} l^+ \\ \swarrow \quad \searrow \\ \text{cross} \\ \swarrow \quad \searrow \\ \bar{\nu}_l \end{array} . \quad (34)$$

The shaded block in Eq. (33) is the full Λp interaction amplitude in cold nuclear matter, which is obtained via dressing a bare Λp interaction by Λ -particles-proton-hole loops

$$\begin{array}{c} \text{shaded box} \\ \text{four arrows} \end{array} = \begin{array}{c} \text{circle} \\ \text{four arrows} \end{array} + \begin{array}{c} \text{loop} \\ \text{shaded box} \\ \text{four arrows} \end{array} , \quad (35)$$

where the bare Λ -proton-hole interaction is presented as

$$\begin{array}{c} \text{circle} \\ \text{four arrows} \end{array} = \begin{array}{c} \text{dotted line} \\ \text{four arrows} \end{array} + \begin{array}{c} \text{cross} \\ \text{four arrows} \end{array} . \quad (36)$$

The dotted line is determined by Eq. (32) and the shaded box represents the short-range Λ -proton-hole interaction, given in Eq. (4).

Calculation of diagrams (31) according to standard diagrammatic rules results in the sum of Eqs (15) and (27). Thus, making use of the optical theorem allows to naturally avoid the double counting problem.

B. Non-strange channel

There are other processes with the positron or positive muon production in neutrino nucleus scattering, supplemented by production of non-strange particles. These give the background to the above considered processes. This background can be in principle subtracted by simultaneous registration of strange particles in the final state. However, even without this experimentally complicated approach, one can hope to detect contributions of processes with strangeness production.

Let us consider the non-strange processes in more detail. Some of them are easily distinguishable from those with strangeness production having different kinematics but the process $\bar{\nu}_l \rightarrow l^+ + \pi^-$ considered in [18] and the related processes $\bar{\nu}_l + p \rightarrow l^+ + n$, $\bar{\nu}_l + N \rightarrow l^+ + \Delta(1232)$, considered in [19,20], occur in the same energy-momentum region. Their probability is rather large.

In terms of the optical theorem formalism these processes can be interpreted as an excitation of in-medium particle-hole and Δ -hole quanta of interaction. As well known, cf. Ref. [15], these quanta are strongly mixed with each other and with in-medium pionic excitations. Thus, in medium these processes should be considered within the optical theorem formalism to prevent a possible double counting. Calculating the rates of the non-strange processes above one has to take into account the weak-interaction renormalization due to the short-range NN and $N\Delta$ correlations.

In Ref. [19,20] these effects were partially included for the $\bar{\nu}_l + p \rightarrow l^+ + n$ channel in the framework of the RPA approximation. The net effect from the correlations is a suppression by the factor $\simeq 0.5$. In the $\bar{\nu}_l + N \rightarrow l^+ + \Delta(1232)$ channel no correlations were included.

We expect that a more consistent account for correlations will lead to a larger suppression effect. Indeed, a rough estimation beyond RPA gives for the reaction $\bar{\nu}_l + p \rightarrow l^+ + n$ the correlation factor, e.g., in the axial current vertex $\gamma_N(g') \simeq 1/(1 + g' 2 m_N^* p_F(\rho_0)/\pi^2)$ at small transverse frequencies and transverse momenta $\sim p_F(\rho_0)$, being the Fermi momentum of a nucleon at the normal nuclear density. Evaluating this expression with $g' \approx 0.7 m_\pi^{-2}$, being the spin-isospin Landau-Migdal parameter of the short-range NN interaction, we find the suppression factor for the reaction rate about $\gamma_N^2(g') \simeq 0.1-0.3$. For the reaction $\bar{\nu}_l + N \rightarrow l^+ + \Delta(1232)$, effects due to the NN and $N\Delta$ correlations are less important, and the resulting suppression factor is expected to be in the range 0.5–0.7.

To compare the rates of strange and non-strange channels of anti-neutrino nucleus scattering we take the results from Ref. [19], the thin dashed curve in Fig. 3, which are close to our calculation with account for the baryon mass reduction due to the mean field interactions. With the suppression factors above we estimate that the strange and non-strange channels give contributions of the same order to the angular integrated cross section. The cross sections taken at the fixed $\bar{\nu}-l^+$ scattering angle correspond to the different kinematics and can be distinguished, thereby.

VII. CONCLUSION

We calculated the differential cross section for the anti-neutrino induced production of positive leptons on a nucleus associated with production of strangeness $S = -1$.

The most important contribution is found to be given by the reaction $\bar{\nu} + p \rightarrow \Lambda + l^+$, which we calculated, including weak-interaction renormalization in nuclear matter due to the short-range Λp correlations taken within Landau–Migdal parameterization. The in-medium effects alter essentially the differential cross section at small $\bar{\nu}$ - l^+ scattering angles both in the absolute value and in the shape. The total cross section changes by $\sim 10\%$.

We also considered a contribution from the in-medium kaon production process $\bar{\nu}_l \rightarrow l^+ + K^-$. For that we evaluated the K^- spectral density in nuclear matter and included the weak-coupling vertex renormalization. The latter increases the rate of positron production in this channel by factor $\sim 10^5$ compared to that estimated with the free weak coupling. In spite of that the contribution of the reaction channel $\bar{\nu}_l \rightarrow l^+ + K^-$ to the full $S = -1$ strange particle rate is $\sim 10^3$ times smaller than that of the reaction $\bar{\nu}_l + p \rightarrow l^+ + \Lambda$. Thus, only a peculiar experimental analysis could allow to discriminate the contribution from this in-medium K^- channel.

We demonstrated that the rate of both reactions $\bar{\nu}_l \rightarrow l^+ + K^-$ and $\bar{\nu}_l + p \rightarrow l^+ + \Lambda$ is not given by the direct sum of the squared matrix elements of the corresponding Feynman diagrams. Otherwise, some processes would be counted twice. We show that this double counting problem is easily avoided in the framework of the optical theorem formalism [10,11]. The closed diagram method, we demonstrated, is quite general and can be applied for any other reaction channels, e.g., for the non-strange reaction channel, which also requires consistent inclusion of in-medium effects.

Both strange and non-strange contributions to the angular integrated cross sections are found to be of the same order of magnitude. However, they are related to the distinct kinematic regions at the fixed neutrino lepton scattering angle. They also can be distinguished with the help of a simultaneous identification of strange particles in the final state.

The developed formalism can be utilized in investigation of other weak processes $e^- \rightarrow K^- + \nu_e$, $e^- + n \rightarrow \Sigma^- + \nu_e$, and $n + n \rightarrow \Lambda + n$ important for neutron star physics, giving rise to hyperonization [3] and K^- condensation [1,2]. The corresponding neutrino radiation can result in some observable consequences, as a jump in neutrino radiation and reheating. The rates of these processes are sensitive to in-medium renormalization of the weak-interaction vertices, Λ -nucleon correlation effects, and to the K^- spectral density as well.

Acknowledgments. The authors would like to thank R. Dahl, M. Lutz and W. Weinhold for discussions and helpful remarks, and the GSI theory group for hospitality and support. The work has been supported in part by BMBF under the program on scientific-technological collaboration (WTZ project RUS-656-96).

REFERENCES

- [1] G.E. Brown, Nucl.Phys. A574, 217c (1994);
C.-H. Lee, G.E. Brown, D.-P. Min, and M. Rho, Nucl. Phys. A585, 401 (1995).
- [2] E.E.Kolomeitsev, D.N. Voskresensky, and B. Kämpfer, Nucl. Phys. A588, 889 (1995).
- [3] N.K. Glendenning, Z. Phys. A327, 327 (1987).
- [4] G.Q. Li and C.M. Ko, Phys. Lett. B349, 405 (1995);
E.L. Bratkovskaya, W. Cassing, and U. Mosel, Nucl. Phys. A622, 593 (1997).
- [5] E.E.Kolomeitsev, D.N. Voskresensky, and B. Kämpfer, Int. J. Mod. Phys. E5, 313 (1996).
- [6] P.B. Siegel, W.B. Kaufmann, and W.R. Gibbs, Phys. Rev. C30, 1256 (1984);
G.E. Brown, C.B. Dover, P.B. Siegel, and W. Weise, Phys. Rev. Lett. 60, 2723 (1988).
- [7] E. Friedman, A. Gal, and C.J. Batty, Nucl. Phys. A579, 518 (1994);
M. Lutz, e-print nucl-th/9802033;
M. Lutz and W. Florkowski, in preparation.
- [8] R.F. Sawyer, Phys. Rev. Lett. 73, 3363 (1994).
- [9] D.N. Voskresensky and A.V. Senatorov, Zh. Eksp. Theor. Fiz. 90, 1505 (1986) [Sov. Phys. JETP 63, 885 (1986)].
- [10] D.N. Voskresensky and A.V. Senatorov, Yad. Fiz. 45, 657 (1987) [Sov. J. Nucl. Phys. 45, 411 (1987)].
- [11] J. Knoll and D.N. Voskresensky, Ann. Phys. 249, 532 (1996).
- [12] T. Waas, N. Kaiser, and W. Weise, Phys. Lett. B365, 12 (1996); Phys. Lett. B379, 34 (1996);
M. Lutz, Phys. Lett. B426, 12 (1998).
- [13] G. Baym, and G.E. Brown, Nucl. Phys A247, 395 (1975);
E. Oset, H. Toki, and W. Weise, Phys Rep. 83, 281 (1982).
- [14] H. Yabu, S. Nakamura, F. Myhrer, and K. Kubodera, Phys. Lett. B135, 17 (1993).
- [15] A.B. Migdal, Rev. Mod. Phys. 50, 107 (1978);
A.B. Migdal, E.E. Saperstein, M.A. Troitsky, and D.N. Voskresensky, Phys. Rep. 192, 179 (1990).
- [16] A.B. Migdal, Zh. Eksp. Theor. Fiz. 61, 2210 (1971) [Sov. Phys-JETP 34, 1184 (1972)];
R. F. Sawyer, Phys. Rev. Lett. 29, 382 (1972);
D.J. Scalapino, Phys. Rev. Lett. 29, 386 (1972).
- [17] N.G. Kelkar, E. Oset, and P. Fernández de Córdoba, Phys. Rev. C55, 1964 (1997).
- [18] R.F. Sawyer and A. Soni, Phys. Rev. Lett. 38, 1383 (1977).
- [19] H. Kim, S. Schramm, and C.J. Horowitz, Phys. Rev. C53, 2468 (1996), Phys. Rev. C53, 3131 (1996).
- [20] H. Kim, J. Piekarewicz, and C.J. Horowitz, Phys. Rev. C51, 2739 (1995).

FIGURES

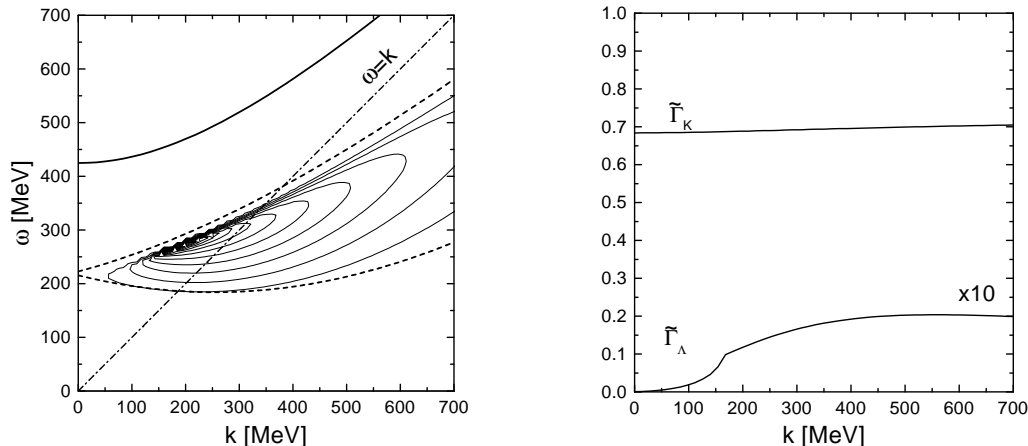


FIG. 1. Spectral density of K^- excitations in isospin symmetrical nuclear matter at $\rho = \rho_0$ (left panel) and the occupation factors of in-medium kaons (right panel). The line $\tilde{\Gamma}_K$ corresponds to the upper kaon branch. The line $\tilde{\Gamma}_\Lambda$ is related to the integral over the region of the Λ -proton-hole continuum between dashed lines on the left plane.

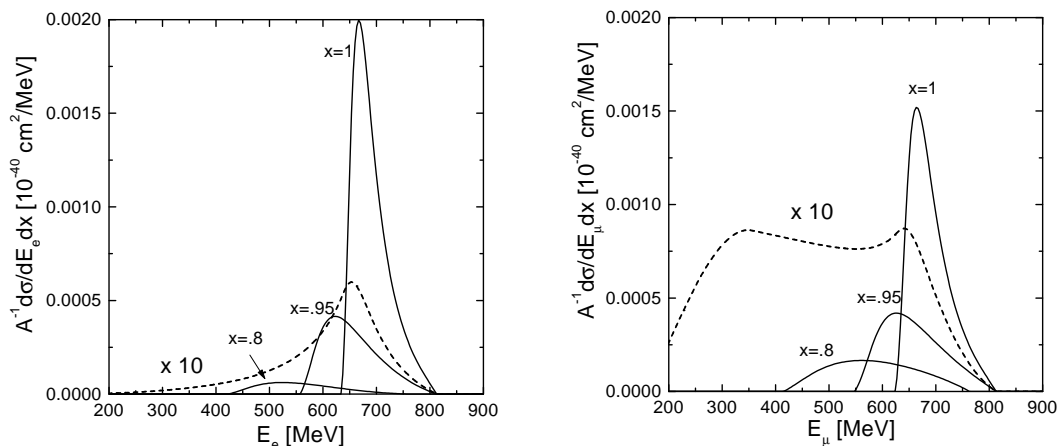


FIG. 2. Differential cross section (per particle) as the function of the lepton energy for positron (left panel) and positive muon (right panel) production in reaction $\bar{\nu}_l \rightarrow l^+ + K^-$ by anti-neutrinos scattering on a nucleus with beam energy 1 GeV. Solid lines are calculated for three values of the scattering angle θ_l between an anti-neutrino and a lepton, labeled by the values of $x = \cos\theta_l$. Dashed lines show the cross section integrated over the lepton angle θ_l .

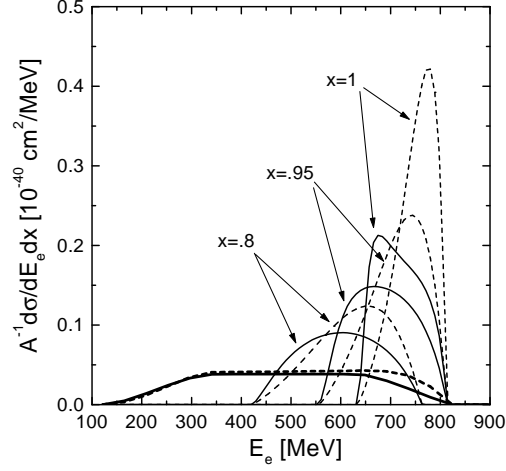


FIG. 3. Differential cross section (per particle) of positrons produced in reaction $\bar{\nu}_l + p \rightarrow l^+ + \Lambda$ by anti-neutrino of beam energy 1 GeV. Thin solid lines correspond to calculations with in-medium vertex renormalization. Thin dashed lines show the result without inclusion of short-range ΛN correlations. Thick solid and dashed lines depict the cross sections integrated over the lepton angle θ_l with and without account for vertex renormalization.